Supplementary Information for Makarenko et al.

PASSIVE STIFFNESS CHANGES DUE TO UPREGULATION OF COMPLIANT TITIN ISOFORMS IN HUMAN DCM HEARTS

Expanded Materials and Methods

Human heart tissue

Left ventricular (LV) samples obtained from human hearts (HH) were classified into two groups: (1) Nonfailing HH-samples (n=19; set1=10, set2=9 hearts) obtained from brain-dead human donors, for which normal LV function had been confirmed by echocardiographic evidence (age range, 43-67 years); echocardiograms were performed within 24 hours prior to the explantation of the heart. (2) Explanted hearts (n=9) from patients diagnosed with severe nonischemic DCM (NYHA class IV), showing clear evidence of LV dysfunction and congestive heart failure, but no signs of ischemia and normal coronary angiograms (age range, 49-65 years). The study was approved by the Subcommittee on Human Research at Massachusetts General Hospital.

The donor hearts were placed *in toto* including both atria, both ventricles and all major vessels intact in University of Wisconsin cardioplegia solution on ice and transported to the Cardiovascular Research Center, Massachusetts General Hospital, Boston. The time of transport of the donor hearts varied between 1-6 hours. The failing hearts were recovered from the surgical suites of Massachusetts General Hospital at the time of cardiac transplantation. Routinely we obtained ~100 grams of tissue from the LV (all walls), right ventricle, and atria. These tissues were also stored for transport in University of Wisconsin solution on ice and the time of transport for the failing hearts was 30 minutes.

LV tissue was dissected in the University of Wisconsin solution on ice. If not indicated otherwise, the anterolateral-midwall region was analyzed. However, in the nine donor hearts of set2 (age range, 48-62 years) we dissected the free LV wall into endocardium, midwall and epicardium. Generally we studied non-fibrotic areas of the heart, as detected by gross examination of the ventricles cut in transverse fashion. After dissection, samples were

quick-frozen in liquid nitrogen and stored at -80°C. The handling of all the hearts was consistent since they were prepared by either R.J.H. or F.d.M. We did not use protease inhibitors or BDM during transport.

As a control, normal HH-tissue was purposely degraded by leaving homogenized sample standing at 25°C in the absence of leupeptin (Fig. 1)—this protease inhibitor is otherwise present in all our buffer solutions—and 2% SDS-polyacrylamide gel electrophoresis (SDS-PAGE) was performed. Within 20 min, the intensity of a "T2" titin-degradation band increased by a factor of >3. T2-titin appeared stronger than the faint T2-bands observable in all HH-samples prepared aiming at maximally preserving the titin. Nevertheless, the band widths and the proportion of N2BA-titin (~32% in the example of Fig. 1) remained more or less constant. Thus, even if titin were somewhat (uncontrollably) degraded during HH-transportation or tissue preparation, the N2BA:N2B ratio is unlikely to be much affected.

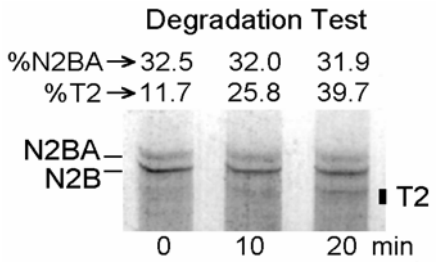

Fig. 1: Titin-band intensities on 2% SDS-polyacrylamide gel of normal HH-tissue allowed to degrade for 10-20min at room temperature in the absence of protease-inhibitor leupeptin. Numbers above lanes indicate percentages of N2BA-titin and T2 (degraded) titin, relative to total N2B+N2BA titin.

In gel-electrophoretic studies on animal hearts we found that titin protein or titin mRNA do not degrade appreciably in the intact heart left standing on ice in cardioplegia solution for several hours without protease inhibitor (unpublished data, 2004). In additional control experiments (Fig. 2), one part of an explanted DCM-HH sample was stored in cardioplegia with protease inhibitor (DCM+Pi) and another part of that heart in cardioplegia without protease inhibitor (DCM-Pi). Titin-protein expression was again analyzed by 2% SDS-PAGE. Fig. 2 shows that the N2BA and N2B-titin bands, as well as the T2 titin-degradation bands, were indistinguishable between DCM+Pi and DCM-Pi HH-samples, indicating that there is no appreciable degradation of titin during transportation and handling of the HH tissue, even if no protease inhibitor is present.

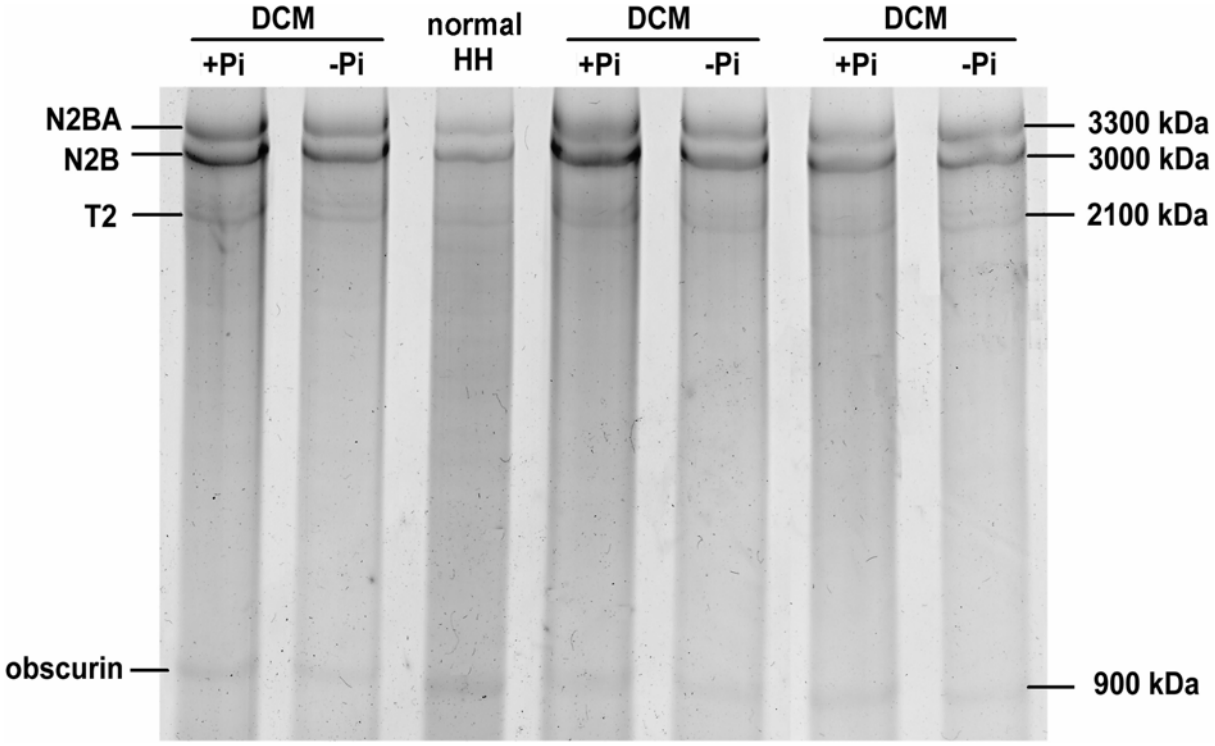

Fig. 2: 2% SDS-polyacrylamide gel to compare the titin bands of DCM-HH samples stored in a solution containing protease inhibitor leupeptin (DCM+Pi) or lacking it (DCM-Pi). A healthy HH-sample (normal HH) is shown for comparison. Both DCM+Pi and DCM-Pi show a broader and more intense N2BA band than the control HH, but there was no difference between DCM+Pi and DCM-Pi.

2% SDS-PAGE

Frozen tissue samples (~20 mg) were quickly homogenized in 200 µl ice-cold solubilization buffer (1% SDS, 1% 2-mercaptoethanol, 10% glycerol, 8 µg/ml leupeptin, 6 µM bromphenol blue, 4.3 mM Tris-HCl, pH 8.8, 4.3 mM EDTA). Samples were incubated for 5 min on ice and then boiled (95°C) for 3 min and centrifuged briefly. The total protein content was determined spectrophotometrically. Lanes on gels were loaded with equal amounts of protein, except when calibration curves were generated.[1] Agarose-strengthened 2% SDS-polyacrylamide gels[2] with a Laemmli-buffer system[3] were prepared to detect titin isoforms with a resolution of <100 kDa.[1,4] If not processed for Western blot, gels were stained with Coomassie brilliant-blue R. In some cases, gels were stained with silver to improve sensitivity. The integrated optical densities of titin bands (Coomassie-stained gels only) were determined on scanned gel images using TotalLab software (Phoretix). The N2BA:N2B titin-isoform ratios were calculated after constructing calibration curves to test for a linear

relationship of titin-band intensity *versus* protein load.[1] This approach provided quite reproducible values: we estimated that, for a given heart sample, the N2BA:N2B ratio was measurable with an error of less than 4% (see Fig. 2B in the main text). The total-titin content per unit tissue was determined by relating the combined titin-band intensities to the total protein content and expressing the mean total-titin content per unit tissue of DCM-hearts relative to that of normal HHs.

Immunoblotting

Immunoblotting was done using chemiluminescent reaction kit (ECL-system, Amersham Pharmacia) according to standard protocols. Blots were also loaded with rabbit soleus tissue, as the titin isoform of this muscle (3.7 MDa) served as a reference band, together with the 3.0 MDa N2B-isoform of human cardiac muscle. Primary titin antibodies were: I17 to cardiac-specific N2-B-region,[5] MG1 to N2-A-region,[6] and BD6 to all titin isoforms.[7] We also used anti-obscurin antibodies I48/I49 kindly provided by Dr. M. Gautel.[8] Peroxidase-conjugated IgG served as secondary antibody.

RT-PCR

RT-PCR primers were designed with a computer program (Primer Express 2.0) to the human genomic sequence of titin (Acc. No. AJ277892).[9] Primer sequences are shown in Table 1. Primers were designed across exon boundaries to ensure that no genomic DNA was amplified. Frozen samples were kept in liquid nitrogen or at -80°C before extraction of total RNA using Trizol (Invitrogen). However, to rule out the possibility of RNA degradation, control qRT-PCR measurements were also performed with human cardiac biopsies which were immediately stored in RNAlater (Ambion). No difference in RNA preservation could be detected between the two methods (data not shown).

Quantitative real-time RT-PCR was performed as described[10] using 25µl SYBR Green PCR Mastermix (Applied Biosystems), 3µl 5µM forward and reverse primer each, 1µl cDNA template and 18µl H_20. Real-time RT-PCR was conducted in an ABI 7000 thermal cycler. The protocol consisted of 2 min at 50°C, 10 min at 95°C and then 40 cycles of incubation at 95°C for 15 seconds followed by one minute at 60°C. Six healthy and six DCM

human hearts were studied; each heart was analyzed at least in triplicate, mostly in quadruplicate. Data acquisition and analysis were performed with ABI Prism 7000 SDS software. The primers specifically amplified the desired products judged from the product lengths (monitored using gel electrophoresis), corresponding to the lengths predicted from titin's genomic sequence if the respective exons are spliced directly to one another. Contamination, mispriming, and the formation of primer-dimer artifacts were ruled out by melting-curve analysis (Fig. 3). Whereas standard curves are widely used for calculating amplification, a recent evaluation of this method showed that it is less erroneous and more practical to directly compare experimental samples against controls.[11]

Table 1: Primers for qRT-PCR.

Exons	**Sense primer (5'-3')**	**Antisense primer (5'-3')**
Ex 49-50	GTAAAAAGAGCTGCCCCAGTGA	GCTAGGTGGCCCAGTGCTACT
Ex 107-108	CAGCAGAACTCAGAATCGA	ATCAAAGGACACTTCACACTC
Ex 50-219	CCAATGAGTATGGCAGTGTCA	TACGTTCCGGAAGTAATTTGC
Ex 50-51	GCCACACTAACTGTGACAGAGG	GGCTGCCTTACCCACAAAAG
Ex 54-55	GGAATTAATAGTTAAAGAACCTGCCAAA	CTCCTGCTGTCACCTGGATCA
Ex 50-60	CCAATGAGTATGGCAGTGTCA	CCGGAGGGAGCTGGTACTC
Ex 50-77	GCTTCCAATGAGTATGGCAGTGT	CGTAACAAAATAAGGCGGTTCTGTC

The amount of a target mRNA was calculated relative to a reference mRNA (mostly total titin) according to:

$$\text{mRNA ratio} = 2^{-[CT(\text{target})-CT(\text{reference})]},$$

where CT is the threshold cycle.[10] The amount of total-titin mRNA (Ex 49-50) in cHHs and DCM-HHs was analyzed relative to an arbitrarily chosen reference, CT (CT=24). The amount of the other splice variants was calculated relative to total titin. The relative values for each titin species were then averaged for the normal and the DCM-HHs, respectively.

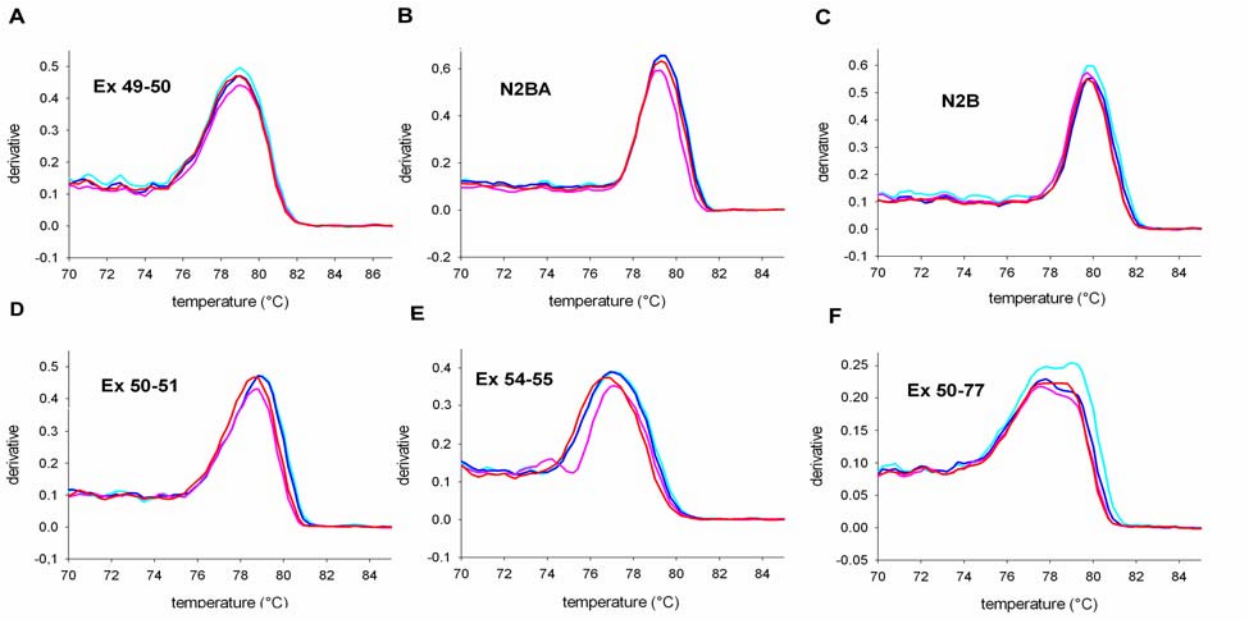

Fig. 3: Typical melting curves of the products amplified by the primer pairs used in the qRT-PCR measurements. Shown are melting curves of the products amplified by primers to (A) total titin, (B) all-N2BA titin, (C) N2B titin, and (D-F) individual N2BA splice variants. Blue and cyan, qRT-PCR products of healthy human hearts; red and pink, qRT-PCR products of DCM human hearts. Ex, exon.

Real-time efficiencies were calculated from the slopes obtained from the ABI 7000 software after performing measurements with cDNA dilutions 1, 0.1, 0.01 and 0.001 using all of the primers. The corresponding real-time PCR efficiency, E, of one cycle in the exponential phase was calculated according to:

$E = 10^{-1/slope}$.

According to the mathematical model of Pfaffl (2001),[12] the relative quantification of a target mRNA in comparison to a reference mRNA was calculated based on E and the difference between the CT of the sample and that of a control. However, SDs could have been determined only by Gaussian approximation with this method. Therefore, the values shown in "Results" were all calculated without correction for the primer efficiencies.

Histology

Small blocks of HH-tissue were incubated in 4% paraformaldehyde overnight. Then the blocks were attached to the plates of a cryosectioning device (MICROM HM 500 O)

using Frozen Section Medium (Neg –50; Richard-Allan Scientific) and frozen to –20°C. The samples were cut into 20µm thick sections and mounted on gelatin-covered slides.

Mallory trichrome stain. Aniline blue/Orange G staining solution was prepared by dissolving 0.5 g Aniline blue (acid blue) (SERVA), 2 g Orange G (Chroma) and 1 g tungstophosphoric acid (MERCK) in 100 ml distilled water. The solution was then filtered using filter paper (Schleicher & Schuell). The sections were stained in 0.25% Fuchsine acid (MERCK) solution for 30 min and dried with paper. Then the sections were stained in Aniline blue/Orange G staining solution for 60 min at 56°C. The sections were dehydrated by different concentrations of ethanol (70, 80, 96 and 100%) (MERCK) for 30 s each and then washed twice for 2 min in xylol (MERCK). Then they were embedded in EUKITT (O. Kindler GmbH), and the microscope slide (Menzel Gläser) was mounted with a coverslip (Menzel Gläser). Images were recorded using a Leitz Orthomat-W microscope with camera attached. The area occupied by cardiomyocytes was measured in seven different DCM-HHs (19 sections) and four different control HHs (8 sections) using ScionImage software.

Myofibril mechanics

Cardiac myofibrils were prepared as described[5,13] from frozen HH-tissue.[1] Briefly, thin muscle strips were dissected in a solution containing (in mM): NaCl 132; KCl 5; EGTA 5; $MgCl_2$ 1; glucose 7; pH 7.1. The muscle strips were tied to thin glass rods and skinned in ice-cold rigor solution, containing (in mM): KCl 75; TRIS 10; EGTA 2; $MgCl_2$ 1 (pH 7.1) in the presence of 0.5% Triton X-100 for ≥4 hours. To obtain individual myofibrils, the skinned strips were minced and homogenized in rigor solution. All solutions were supplemented with 40 µg/ml protease inhibitor leupeptin to minimize titin degradation. Elsewhere we reported that freezing does not alter the passive mechanical properties of heart samples.[14]

A setup for myofibrillar force measurements has been described.[2] Briefly, under a Zeiss Axiovert 135 microscope, a myofibril is suspended between micromanipulator-positioned glass needles attached to a piezoelectric actuator (Physik Instrumente, Karlsruhe, Germany) and a fibre optic-based force transducer (homebuilt) with nanonewton resolution. Attachment of the myofibrils is aided by coating the needle tips with a water-curing silicone adhesive (2:1 (v/v) mixture of Dow Corning 3145 RTV and 3140 RTV). Data collection and motor control were done with a PC, DAQ board, and custom-written LabView software

(National Instruments). Myofibril images were recorded with a color-CCD camera (Sony), frame grabber, and Scion Image software (NIH, Bethesda, MD) or with a linear photodiode array, PC, DAQ board and LabView algorithms.[14]

Force measurements were carried out at 25°C in relaxing buffer supplemented with 30 mM 2,3-butanedione monoxime (an active-force inhibitor) and 40 μg/ml protease inhibitor leupeptin.[2,14] Force was sampled at 1 kHz. Two different protocols were performed. In the first, force was recorded during stepwise stretch of myofibrils from slack sarcomere length (SL) to a maximum SL of 2.4 μm. The stretch amplitude per step was 0.1 μm/sarcomere. Each step lasted 1 s, followed by a 19-s hold period. After the last stretch-hold, myofibrils were released in larger steps back to slack SL, to test for possible shifts of baseline tension. Six identical stretch-release protocols were performed on a myofibril and data were averaged to improve the signal-to-noise ratio. In the force recordings, we distinguished peak (total) tension at the end of each stretch, decaying (viscous/viscoelastic) tension during each hold period, and elastic tension at the end of each hold period. The passive elastic-force component of the cardiac sarcomere is due to the elasticity of titin,[15] whereas the viscous/viscoelastic components have multiple sources, including actin-titin interactions.[13,14] At SLs above approximately 2.2 μm, a quasi-steady-state elastic force was not yet reached during the 19-s hold period. Therefore, the elastic force component was determined from a three-order exponential decay fit applied to the decay-force trace (Fig. 4).[16]

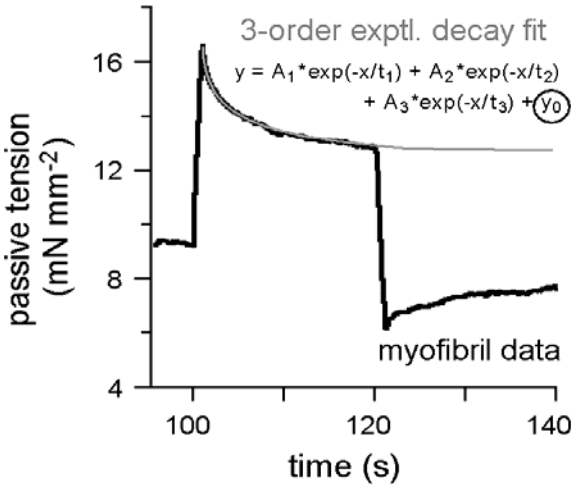

Fig. 4: Exponential decay fit to stress relaxation data obtained from cardiac myofibrils, to determine quasi-steady-state elastic force (y_o).

In the second protocol, force was recorded during triangular stretch-release movements; each cycle lasted 1 s (Fig. 5). The SL-range covered was 1.85 µm (slack SL) to 2.4 µm. Ten consecutive loops were applied and then a one-minute pause was observed; the protocol was repeated 8 times and force traces were found to be reproducible. From averaged force traces, hysteresis (the PT-difference between stretch and release curves) was calculated as the area between the stretch and release curves of a given cycle. Measured force values were normalized to the myofibrillar cross-sectional area.[2] The analysis revealed that hysteresis drops quickly to reach ~60% of the initial value after five cycles, but changes little thereafter (Fig. 5, inset). This result prompted us to analyze the force data obtained in the 5th loop in the passive-tension measurements on HH-fiber bundles (see next section), but skip the data of the first four cycles (Fig. 7 in main text).

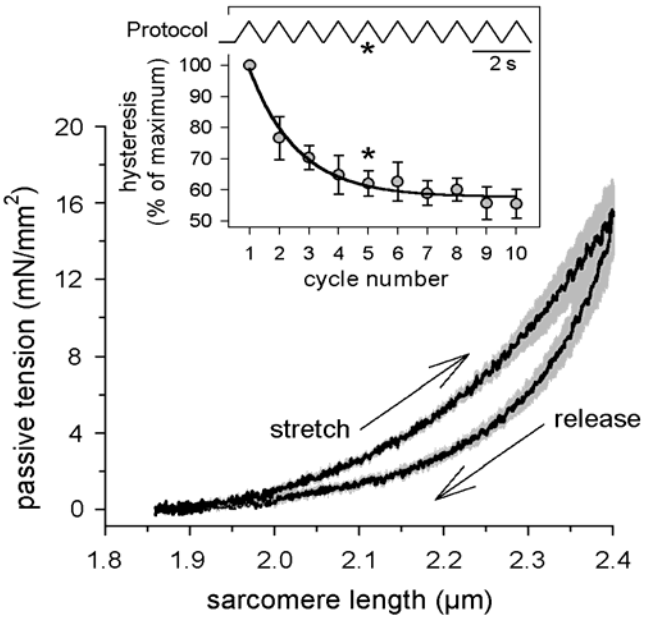

Fig. 5: Passive tension of isolated cardiac myofibrils (normal HH). Black curve is mean of three myofibrils, grey shade is SEM. PT-data shown were obtained during the 5th, out of 10, stretch-release cycles. Inset: Experimental protocol and change in hysteresis (the area between stretch-curve and release-curve) with stretch cycle number; data are mean±SEM; n=3; asterisks indicate 5th loop.

Passive force measurements on human heart fiber bundles

Frozen LV tissue from normal donor hearts and DCM HHs was dissected into strips approximately 400-500 µm in diameter and 3-4 mm long. Care was taken to dissect the fiber bundles in the direction of the fibers and to avoid stretching the preparations during dissection. Muscle strips were skinned in relaxing solution containing 1% w/v Triton X-100

overnight on ice, as described in Ref. 17. After skinning, the fiber bundles were washed thoroughly with relaxing solution. All buffers contained 40 µg/ml protease inhibitor leupeptin.

Mechanical measurements were made with a workstation for muscle mechanics (Scientific Instruments, Heidelberg)[1,14] at room temperature. Besides leupeptin, relaxing buffer also contained 30mM BDM. Preparations were attached to the motor arm and to the force transducer by the company-made stainless steel clips. The diameter of each sample (in the non-stretched state) was measured using a binocular microscope. The diameter was used to calculate the cross-sectional area and the force per unit area. In addition, fiber bundles were fixed with 4% paraformaldehyde in relaxing buffer following the mechanical measurements and cross-sections were cut with a microtome (Fig. 6). The cross-sectional area was determined in at least five sections cut along the fiber axis; the area varied by less than 15% among different sections of the same muscle strip. The cross-sectional area generally was of near-circular shape (Fig. 6). The measured areas compared reasonably well with the values calculated, as described above, from the diameter of the preparations.

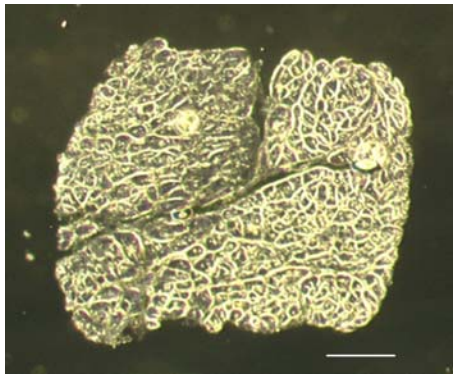

Fig. 6: Cross-section of a typical fiber bundle. Fiber bundles of human heart, as shown here in cross section, were used for the passive mechanical measurements, and cross-sectional area was checked on tissue sections. Fiber bundles were chosen in order to measure the passive stiffness of both intracellular and ECM material such as collagen. Bar, 100 µm.

Sarcomere length was measured by laser diffraction.[1,14] If the diffraction pattern was too noisy to reliably measure SL—due to the thickness of the sample—the strip was stretched from slack length (corresponding to 1.80-1.85 µm SL in all fibers in which a clean diffraction pattern did allow SL-detection) by a predetermined amplitude of 30% the initial muscle length. This stretch amplitude fully covers the physiological SL-range of approximately 1.8 to 2.4 µm. The experimental protocol followed one described by others.[17] Passive force was

measured while stretching the preparation at a constant velocity from slack SL to ~2.40 μm SL, followed by a release at the same velocity. Five consecutive stretch-release cycles (each cycle lasting 1s) were applied, before a rest period of ~2min was observed. Force was analyzed in the 5th loop, when hysteresis had dropped to quasi-stable levels. In both normal-donor and DCM samples, titin was degraded by treating muscle strips with 0.25 μg/ml trypsin for up to 40 min,[17] while stretch-release cycles were recorded at 2-min intervals. Low doses of trypsin have been shown to degrade titin selectively.[18] Titin degradation in HH-fibers by low-dose trypsin was confirmed by 2% gel electrophoresis. After titin degradation, we also added a protocol to extract thin and thick filaments, the anchorage points of titin, by applying 0.6 M KCL followed by 1.0 mM KCL in relaxing solution.[17] Passive tension changed only little during this additional protocol of titin de-functionalization (data not shown).

Modeling titin-based elastic tension based on SDS-PAGE results and mechanical parameters of titin-domain function established by single-molecule analysis

On scanned gels, image-processing was performed using TotalLab software (Phoretix), involving background subtraction and the generation of intensity profiles taken along the center of each gel lane (mean average intensity across a 20-30 pixel-wide segment). Further analysis on the profiles was performed using custom-written routines in Matlab. Calibration for molecular weight was done using a log-log fit to intensity peaks for known bands corresponding to rabbit soleus muscle titin (M_w=3.7 MDa) and the rat heart N2-B titin isoform (M_w≈2.97 MDa) run on the same gel. Edge effects on gels, manifest as a characteristic smiling shape, sometimes resulted in unreliable estimates for absolute molecular weight. However, associating the lower molecular weight titin peak observed in both normal and DCM human heart samples with the N2B isoform allowed the lower molecular weight peak to be fixed, giving very precise estimates for shifts in molecular weight from this value.

Initial fits to the N2B-intensity peak suggested that it could be modelled adequately with a single Gaussian. In contrast, the intensity peak associated with the N2BA isoforms required at least two Gaussians for a reasonable fit, suggesting the presence of at least two N2BA isoforms. The N2BA-Gaussians were assumed to correspond to isoforms due to different insertions of PEVK and Ig-domains (see below). Intensity profiles for normal and DCM human heart titins including both the N2B and N2BA peaks were then fitted with a 3-Gaussian model using a Nelder-Mead Simplex minimization algorithm[19] with the only

constraint that the lowest molecular-weight Gaussian be fixed (corresponding to the N2B titin isoform). For normal hearts the centers of the other two Gaussians were found to range from 3.22 to 3.23 MDa and 3.31 to 3.32 MDa; DCM hearts had an equivalent range of 3.22 to 3.26 and 3.31 to (in some cases) 3.53 MDa, a clear shift towards higher molecular weight isoforms. Estimates for the relative proportions of each titin isoform present were based on the area A_i under each individual Gaussian, which similarly suggested increased expression of higher molecular weight N2BA isoforms for DCM hearts compared to normal. The summation of these areas was found to vary by up to 20% between individual profiles, but no statistically significant difference could be found between normal and DCM.

Predictions for the shape of the force-extension curve of a given titin isoform were based on the assumption that overall single-molecule titin elasticity could be modeled as three independent worm-like chains[20] acting in series, corresponding to segments of tandem-Ig, the PEVK region and the N2-B region.[15] These segments are characterized by different contour and persistence lengths, namely the total titin extension is given by:

$$X = \sum_{i=1}^{3} x_i$$

where the extension x_i at a force F of the i-th spring satisfies:

$$F = \frac{k_B T}{L_{pi}} \left(\frac{1}{4\left(1 - x_i / L_{ci}\right)^2} + \frac{x_i}{L_{ci}} - \frac{1}{4} \right)$$

where k_B is the Boltzmann constant, T the absolute temperature, with L_{pi} and L_{ci} the persistence and contour lengths, respectively, of the i-th spring. Solutions for the equations were found using a standard numerical interpolation technique. Using the same model as Ref.14, unfolding of Ig domains was modeled as a 2-state process (folded and unfolded) for proximal Ig's, with a probability of $P_{prox}=A/(A+B)$, where A and B are force-dependent unfolding and folding rate constants. Unfolding of distal Ig-domains was modeled as a 3-state process (folded, intermediate and unfolded), with a probability of $P_{dist}=A_1A_2/(A_1A_2+B_1B_2+A_1B_2)$, with A_1 and B_1 being force-dependent unfolding and folding rate constants between the fully-folded state and an intermediate state; A_2 and B_2 are the equivalent rate constants between the intermediate state and the fully-unfolded state. The values of parameters used are shown in Table 2. Upon unfolding of an Ig domain the contour

length of the tandem-Ig wormlike chain is assumed to decrease by 4.4 nm, the length of a single folded Ig,[21] with a simultaneous increase in the contour length of the N2-B worm-like chain of 32.5 nm. The result is three different functional force-extension relations, $F_i(X)$.

The increase in molecular weight from the N2B to the N2BA isoforms was assumed to be due to extra insertions of either PEVK or Ig domains. The additional quantity of PEVK for all N2BA isoforms was assumed to be constant at 600 residues.[9] This allowed an estimate for the total Ig domain insertion assuming 10-12 kDa for each extra Ig domain, suggesting that the two main N2BA isoforms contain between 16-20 and 23-29 additional Ig's.

In predicting the shape of the passive tension (T_P) curve for an isolated cardiac myofibril it was assumed that all titin molecules extend independently and non-cooperatively of each other and all in parallel to the longitudinal axis of the myofibril. The total force at each given extension was assumed to be a sum of the three force-extension relations predicted from the previous analysis, weighted in proportion to the relative areas under each individual Gaussian, and all multiplied by a scaling-factor N equivalent to the cross-sectional packing density of titin in the myofibril. Existing myofibril stretch data (elastic component of passive tension) were fitted with the weighted-sum force-extension relation multiplied by a variable scaling-factor with a small variable extension offset X_{offset} to account for imprecision in sarcomere-length measurements, using Nelder-Mead Simplex minimization:

$$SL = n \cdot \lambda \cdot \frac{\sqrt{A^2 + B^2}}{A}$$

Excellent fits were obtained with an extension offset of –30 nm and scaling-factor equivalent to 2.2×10^9 titin molecules/mm^2, very close to the value 2.4×10^9 titin molecules/mm^2 obtained from EM data.[22]

The viscous/viscoelastic passive-force component of isolated human cardiac myofibrils (see Fig. 6 in the main text) was not tried to be modeled, as it has multiple sources.[13,14]

TABLE 2. Parameters used in the prediction of the force-extension relations.

N2B titin isoform

	$A/\ s^{-1}$	$B/\ s^{-1}$	$A_1/\ s^{-1}$	$B_1/\ s^{-1}$	$A_2/\ s^{-1}$	$B_2/\ s^{-1}$	n	L_p/ nm	L_c/ nm
proximal Ig's	-	-	1.0×10^{-2}	100	3.3×10^{-3}	0.33	15	10	66
distal Ig's	8.0×10^{-5}	1.2	-	-	-	-	22	10	97
mid Ig's (N2-B)	8.0×10^{-5}	1.2	-	-	-	-	4	10	18
PEVK	-	-	-	-	-	-	186	0.91	67
N2-B us	-	-	-	-	-	-	572	0.66	206

N2BA titin isoforms

*	$A/\ s^{-1}$	$B/\ s^{-1}$	$A_1/\ s^{-1}$	$B_1/\ s^{-1}$	$A_2/\ s^{-1}$	$B_2/\ s^{-1}$	n	L_p/ nm	L_c/ nm
proximal Ig's	-	-	1.0×10^{-2}	100	3.3×10^{-3}	0.33	15	10	66
distal Ig's	8.0×10^{-5}	1.2	-	-	-	-	22	10	97
mid Ig's	8.0×10^{-5}	1.2	-	-	-	-	20-33	10	88-145
PEVK	-	-	-	-	-	-	786	0.91	283
N2-B us	-	-	-	-	-	-	572	0.66	206

* The number (n) of extra mid Ig's has been deduced by assuming that the extra molecular weight after inclusion of additional PEVK of 600 a.a. for the N2BA titin isoforms is due solely to additional Ig domains. Contour lengths for the PEVK and N2-B regions have been calculated on the basis of 0.36 nm per residue, with contour length for the Ig regions being 4.4 nm per domain. Since the persistence lengths for distal and proximal are equal they can be represented as a single wormlike chain whose contour length is the sum of those for the two separate regions. For the model, mid Ig's were assumed to have properties equivalent to distal Ig's. All kinetic parameters taken from data published in Ref. 15.

REFERENCES

1. Neagoe C, Kulke M, del Monte F, Gwathmey JK, de Tombe PP, Hajjar RJ, Linke WA. Titin isoform switch in ischemic human heart disease. *Circulation.* 2002;106:1333-1341.
2. Linke WA, Ivemeyer M, Labeit S, Hinssen H, Rüegg JC, Gautel M. Actin-titin interaction in cardiac myofibrils: probing a physiological role. *Biophys J.* 1997;73:905-919.
3. Tatsumi R, Hattori A. Detection of giant myofibrillar proteins connectin and nebulin by electrophoresis in 2% polyacrylamide slab gels strengthened with agarose. *Anal Biochem.* 1995;224:28-31.
4. Neagoe C, Opitz CA, Makarenko I, Linke WA. Gigantic variety: expression patterns of titin isoforms in striated muscles and consequences for myofibrillar passive stiffness. *J Muscle Res Cell Motil.* 2003;24:175-189.
5. Linke WA, Rudy DE, Centner T, Gautel M, Witt C, Labeit S, Gregorio CC. I-band titin in cardiac muscle is a three-element molecular spring and is critical for maintaining thin filament structure. *J Cell Biol.* 1999;146:631-644.
6. Gautel M, Goulding D. A molecular map of titin/connectin elasticity reveals two different mechanisms acting in series. *FEBS Lett.* 1996;385:11-14.
7. Whiting A, Wardale J, Trinick J. Does titin regulate the length of muscle thick filaments? *J Mol Biol.* 1989;205:263-268.
8. Young P, Ehler E, Gautel M. Obscurin a giant sarcomeric Rho guanine nucleotide exchange factor protein involved in sarcomere assembly. *J Cell Biol.* 2001;154:123-136.
9. Freiburg A, Trombitas K, Hell W, Cazorla O, Fougerousse F, Centner T, Kolmerer B, Witt C, Beckmann JS, Gregorio CC, Granzier H, Labeit S. Series of exon-skipping events in the elastic spring region of titin as the structural basis for myofibrillar elastic diversity. *Circ Res.* 2000;86:1114-1121.
10. Opitz CA, Leake MC, Makarenko I, Benes V, Linke WA. Developmentally regulated switching of titin size alters myofibrillar stiffness in the perinatal heart. *Circ Res.* 2004;94:967-975.
11. Peirson SN, Butler JN, Forster RG. Experimental validation of novel and conventional approaches to quantitative RT-PCR data analysis. *Nucleic Acids Res.* 2003; 31:e71.
12. Pfaffl MW. A new mathematical model for relative quantification in real-time RT-PCR. *Nucleic Acids Res.* 2001;29:2001-2007.

13. Kulke M, Fujita-Becker S, Rostkova E, Neagoe C, Labeit D, Manstein DJ, Gautel M, Linke WA. Interaction between PEVK-titin and actin filaments: origin of a viscous force component in cardiac myofibrils. *Circ Res.* 2001;89:874-881.

14. Opitz CA, Kulke M, Leake MC, Neagoe, Hinssen H, Hajjar RJ, Linke WA. Damped elastic recoil of the titin spring in myofibrils of human myocardium. *Proc Natl Acad Sci USA.* 2003;100:12688-12693.

15. Li H, Linke WA, Oberhauser AF, Carrion-Vazquez M, Kerkvliet JG, Lu H, Marszalek PE, Fernandez JM. Reverse engineering of the giant muscle protein titin. *Nature.* 2002;418:998-1002.

16. Minajeva A, Kulke M, Fernandez JM, Linke WA. Unfolding of titin domains explains the viscoelastic behavior of skeletal myofibrils. *Biophys J.* 2001;80:1442-1451.

17. Wu Y, Cazorla O, Labeit D, Labeit S, Granzier H. Changes in titin and collagen underlie diastolic stiffness diversity of cardiac muscle. *J Mol Cell Cardiol.* 2000;32:2151-2162.

18. Helmes M, Lim CC, Liao R, Bharti A, Cui L, Sawyer DB. Titin determines the Frank-Starling relation in early diastole. *J Gen Physiol.* 2003;121:97-110.

19. Nelder JA, Mead R. A simplex method for function minimization. *Computer J.* 1965;7:308-313.

20. Marko JF, Siggia E. Stretching DNA. *Macromolecules* 1995;28:209-212.

21. Pfuhl M, Gautel M, Politou AS, Joseph C, Pastore A. Secondary structure determination by NMR spectroscopy of an immunoglobulin-like domain from the giant muscle protein titin. *J Biomolec NMR.* 1995;6:48-58.

22. Liversage AD, Holmes D, Knight PJ, Tskhovrebova L, Trinick J. Titin and the sarcomere symmetry paradox. *J Mol Biol.* 2001;305:401-409.